

CTA with Fluoroscopy Image Fusion Guidance in Endovascular Complex Aortic Aneurysm Repair

A.M. Sailer ^{a,*}, M.W. de Haan ^a, A.G. Peppelenbosch ^b, M.J. Jacobs ^b, J.E. Wildberger ^a, G.W.H. Schurink ^b

^a Department of Radiology, Maastricht University Medical Centre, Maastricht, The Netherlands

^b Department of Surgery, Maastricht University Medical Centre, Maastricht, The Netherlands

WHAT THIS PAPER ADDS

The use of CTA with fluoroscopy image fusion guidance for complex endovascular aortic aneurysm repair has been evaluated. Image fusion technology proved to significantly reduce procedure time and volume of iodinated contrast material. A non-significant reduction in fluoroscopy time was observed. Respiration-related vessel displacement and straightening of elongated vessel segments by stiff devices are currently the main limitations in fusion image overlay accuracy.

Objectives: To evaluate the effect of intraoperative guidance by means of live fluoroscopy image fusion with computed tomography angiography (CTA) on iodinated contrast material volume, procedure time, and fluoroscopy time in endovascular thoraco-abdominal aortic repair.

Methods: CTA with fluoroscopy image fusion road-mapping was prospectively evaluated in patients with complex aortic aneurysms who underwent fenestrated and/or branched endovascular repair (FEVAR/BEVAR). Total iodinated contrast material volume, overall procedure time, and fluoroscopy time were compared between the fusion group ($n = 31$) and case controls ($n = 31$). Reasons for potential fusion image inaccuracy were analyzed.

Results: Fusion imaging was feasible in all patients. Fusion image road-mapping was used for navigation and positioning of the devices and catheter guidance during access to target vessels. Iodinated contrast material volume and procedure time were significantly lower in the fusion group than in case controls (159 mL [95% CI 132–186 mL] vs. 199 mL [95% CI 170–229 mL], $p = .037$ and 5.2 hours [95% CI 4.5–5.9 hours] vs. 6.3 hours [95% CI 5.4–7.2 hours], $p = .022$). No significant differences in fluoroscopy time were observed ($p = .38$). Respiration-related vessel displacement, vessel elongation, and displacement by stiff devices as well as patient movement were identified as reasons for fusion image inaccuracy.

Conclusion: Image fusion guidance provides added value in complex endovascular interventions. The technology significantly reduces iodinated contrast material dose and procedure time.

© 2014 European Society for Vascular Surgery. Published by Elsevier Ltd. All rights reserved.

Article history: Received 27 September 2013, Accepted 20 December 2013, Available online 30 January 2014

Keywords: Multimodality image fusion, FEVAR/BEVAR, Road-map, Iodinated contrast material, Computed tomography angiography, Fluoroscopy

INTRODUCTION

Multimodality image fusion guidance is a new alternative to conventional angiogram road-mapping in endovascular interventions. The technology follows two principles:¹ (a) to co-register and fuse pre-acquired image datasets (e.g. computed tomography angiography [CTA] or magnetic resonance angiography [MRA]) with another dynamic imaging modality, commonly fluoroscopy; (b) to overlay real-time catheter and guidewire movements to the pre-acquired background dataset. Rigid co-registration is performed by

means of a C-arm cone beam computed tomography (CBCT) system, allowing the pre-acquired dataset to follow any rotation of the C-arm and table movement. Recently, fusion image road-mapping has been evaluated for cardiologic interventions and in endovascular surgery.^{2–6} Nevertheless, broad application of this technique for routine practice and evaluation of added value and limitations has yet to happen. The purpose of this work was to evaluate the effect of real-time fluoroscopy with CTA image fusion guidance on iodinated contrast material usage, procedure time, and fluoroscopy time in branched and fenestrated repair of complex aortic aneurysms. We further aimed to analyze and quantify limitations of fusion road-map accuracy.

MATERIALS AND METHODS

Image fusion technology was prospectively evaluated for intraprocedural road-mapping in 31 patients with complex

* Corresponding author. A.M. Sailer, Department of Radiology, Maastricht University Medical Centre (MUMC), P. Debyelaan 25, 6229 HX Maastricht, The Netherlands.

E-mail address: anni.sailer@mumc.nl (A.M. Sailer).

1078-5884/\$ — see front matter © 2014 European Society for Vascular Surgery. Published by Elsevier Ltd. All rights reserved.

<http://dx.doi.org/10.1016/j.ejvs.2013.12.022>

aortic aneurysms who underwent fenestrated and/or branched endovascular repair (FEVAR/BEVAR) between March 2012 and September 2013. The study was approved by the institutional ethics committee and the requirement for informed consent was waived by the IRB. Prior to the intervention, all patients had undergone outpatient diagnostic CTA scans on a second-generation dual-source CT scanner (Somatom Definition, Siemens Healthcare, Forchheim, Germany) for measurements and planning of the custom-made endografts. The CTA scans were carried out in dual-energy settings, allowing for dedicated post-processing, including automated bone removal. The endovascular procedure was performed in our hybrid operating theater. Just before surgical vascular access was obtained, an abdominal non-contrast-enhanced CBCT was performed by rotational movement of the C-arm covering a 180-degree circular trajectory (Allura Xper FD20, Philips Healthcare, Best, The Netherlands). Standard parameters for CBCT were 123 kV and additional filtration of 0.9 mm of copper plus 1 mm of aluminum. The volumetric dataset of a total of 316 images was automatically transferred to a 3D workstation (Philips

Allura XtraVision 8.3) and co-registered to patients' pre-interventional diagnostic CTA images. Arterial vessel wall calcifications and bone borders were used as landmarks. During the intervention, the fusion road-map was presented in real-time on a screen next to conventional fluoroscopy.

Fusion image road-mapping was used for navigation and positioning of the stent graft. Before deployment, the accuracy of the fusion road-map and correct position of the stent graft were evaluated by conventional angiography. For catheterization of fenestrations, branches and target vessel, optimal C-arm projection angles were identified on the fusion road-map and access was obtained using fusion guidance. After catheterization, the correct position was tested by catheter injection.

Case—controls

In our clinic, more than 150 FEVAR and BEVAR procedures have been performed since 2006. All of these procedures were performed by the same vascular surgeon together with the same interventional radiologist (last and second

Table 1. Aneurysm characteristics and FEVAR/BEVAR design in the fusion and case—control groups.

Fusion group				Case—control group			
Patient ID	Type of aneurysm	No. of fenestrations (F)/branches (B)	Bifurcated endovascular graft	Patient ID	Type of aneurysm	No. of fenestrations (F)/branches (B)	Bifurcated endovascular graft
1	TAAA I	4 B	No	32	TAAA I	4 B	No
2	TAAA III	3 F/1 B	No	33	TAAA IV	4 F	No
3	TAAA IV	3 B	No	34	Juxtarenal AAA	3 F	No
4	Juxtarenal AAA	4 F	Yes	35	TAAA IV	3 F/1 B	Yes
5	TAAA I	2 F	No	36	TAAA I	2 F	No
6	TAAA III	4 B	No	37	TAAA IV	4 B	No
7	TAAA III	4 F	No	38	TAAA IV	4 F	No
8	TAAA I	3 F/1 B	Yes	39	TAAA II	1F/3 B	Yes
9	TAAA III	6 B	Yes	40	TAAA II	4 B	Yes
10	TAAA III	2 F/2 B	No	41	TAAA IV	4 F	No
11	Juxtarenal AAA	3 F	Yes	42	Juxtarenal AAA	3 F	Yes
12	TAAA II	4 B	No	43	TAAA II	4 B	Yes
13	TAAA II	4 B	Yes	44	TAAA II	4 B	Yes
14	TAAA III	4 B	Yes	45	TAAA III	1F/3 B	No
15	TAAA III	4 B	No	46	TAAA II	4 B	No
16	TAAA IV	3 F	Yes	47	TAAA IV	4 B	Yes
17	Juxtarenal AAA	3 F	Yes	48	Juxtarenal AAA	3 F	Yes
18	TAAA I	4 F	No	49	TAAA I	4 B	No
19	Juxtarenal AAA	3 F	Yes	50	Juxtarenal AAA	3 F	Yes
20	TAAA IV	4 F	Yes	51	TAAA IV	4 B	Yes
21	TAAA I	4 B	No	52	TAAA I	4 B	No
22	TAAA IV	3 F	Yes	53	TAAA IV	3 F	Yes
23	TAAA III	3 F/1 B	No	54	TAAA IV	4 F	No
24	Juxtarenal AAA	3 F	No	55	Juxtarenal AAA	3 F	No
25	Iliac aneurysm	1 B	Yes	56	Iliac aneurysm	1 B	Yes
26	Juxtarenal AAA	3 F	Yes	57	Juxtarenal AAA	3 F	yes
27	TAAA III	3 F/1 B	Yes	58	TAAA III	1F/3 B	Yes
28	Juxtarenal AAA	1 F	No	59	Juxtarenal AAA	2 F	No
29	Juxtarenal AAA	3 F	Yes	60	Juxtarenal AAA	3 F	Yes
30	TAAA V	2 F/2 B	No	61	TAAA IV	4 F	No
31	TAAA III	2 F/2 B	No	62	Juxtarenal AAA	2 F	No
Total number F/B		61 F/51 B		Total number F/B:		56 F/51 B	

Note. TAAA = type of thoraco-abdominal aortic aneurysm according to Crawford classification.

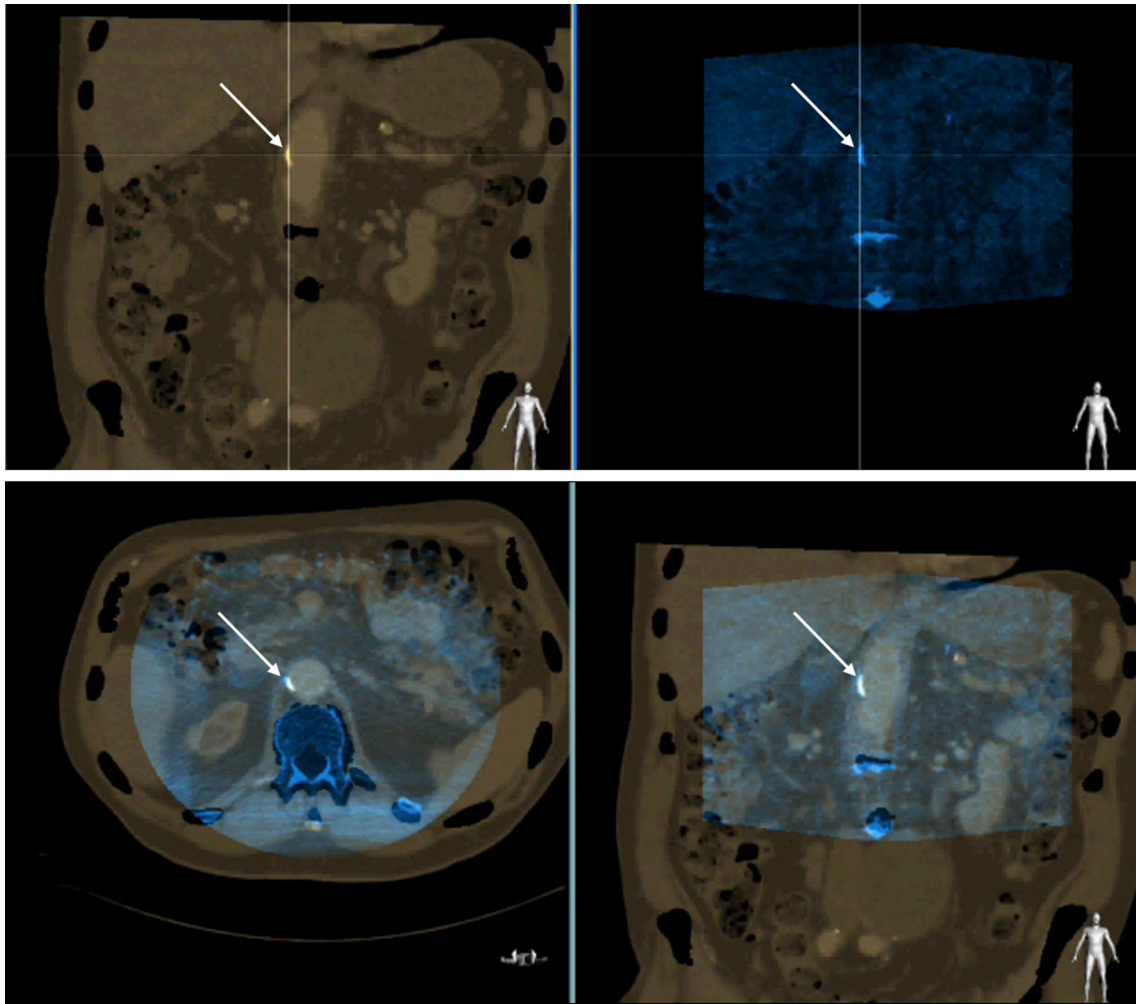


Figure 1. Three dimensional co-registration of volumetric pre-acquired computed tomography angiography (CTA) dataset (grey) with cone beam computed tomography (CBCT) dataset (blue). Top row: Aortic wall calcifications (white arrows) on CBCT and CTA datasets are selected as landmarks and marked with the crosshair. Bottom row: The fused dataset is further adjusted in three dimensions by scrolling through the dataset and aligning bone borders and other calcifications (sagittal plane not shown).

author). Patients undergoing FEVAR/BEVAR between March 2012 and September 2013 were consecutively included in the fusion guidance group. Due to maintenance/software updates, the fusion technology was not available in October 2012 and between April and May 2013; procedures during this period were included in the case–control group. Cases and controls were collected from our historical pool of FEVAR/BEVAR procedures without fusion guidance and limited to the period between 2010 and 2013. Cases and controls were technically comparable in procedure complexity expressed in type of aneurysm (type of TAAA according to Crawford classification, juxtarenal AAA, and one iliac aneurysm), number of fenestrations, and branches as well as presence or absence of a bifurcated endovascular graft. Where more than one case control matched the fusion case, the more recent procedure was included.

Outcome parameters

The radiation dose of CBCT in terms of dose–area product (DAP, in $\text{mGy}\cdot\text{m}^2$) was registered. The total volume of procedural iodinated contrast material (iopromide, 300 mg/mL;

Ultravist, Bayer HealthCare, Berlin) and overall procedure time were registered and compared with data from the case–controls. For the last 22 procedures, fluoroscopy time was also registered and compared with available case–control data. Reasons for potential fusion road-map inaccuracies were analyzed and quantified by the multidisciplinary team.

Statistical analysis

For continuous variables, the *t* test for independent samples or the Wilcoxon test was used for normally and non-normally distributed data respectively (SPSS statistics 20.0, Chicago, IL, USA). Two sided $p < .05$ were considered significant. Quantitative values are presented by means and 95% confidence intervals.

RESULTS

The fusion group consisted of 26 men and five women, with a mean age of 74 ± 6 years. The demographics of the fusion ($n = 31$) and case–control groups ($n = 31$) were similar. An

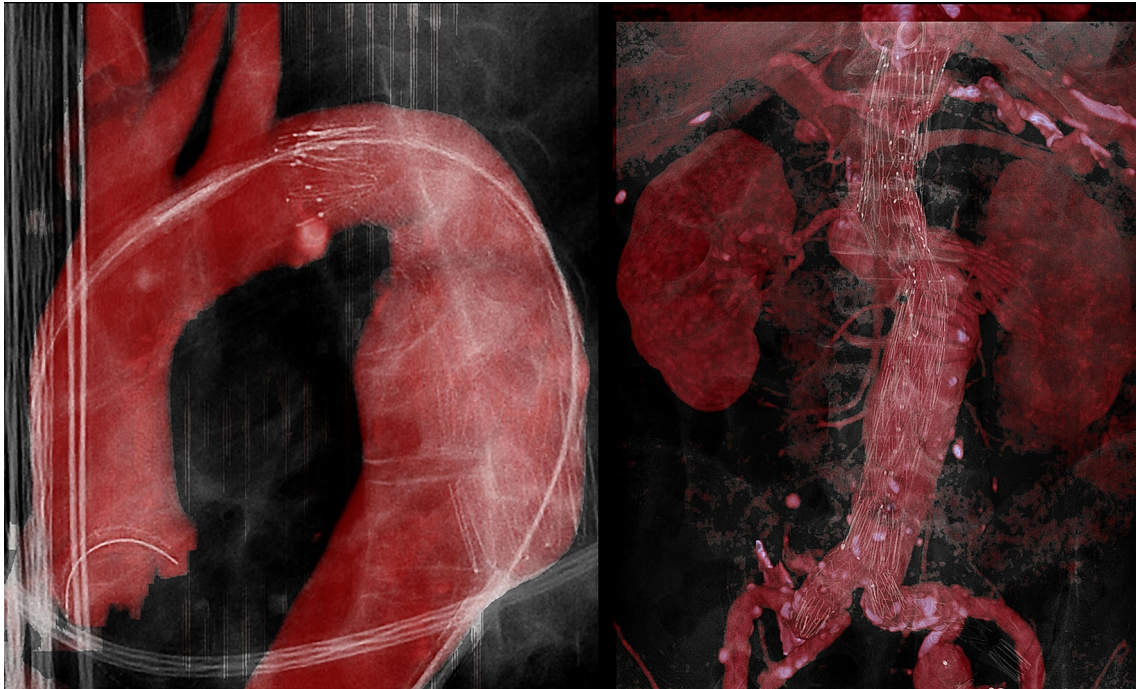


Figure 2. Stent graft placement based on fusion road-map after control for correct overlay position on conventional angiogram. Live fluoroscopy image with main body grafts (white) overlaid on pre-acquired computed tomography angiography background (red) in two different patients.

accurate case–control match for every fusion patient was retrieved on the basis of aneurysm and endograft characteristics. Detailed information on aneurysm type and endograft design for fusion and control patients is shown in [Table 1](#). Mean radiation dose of CBCT was 1.43 mGy² (95% CI 1.20–1.66 mGy²). Image co-registration and fusion guidance were feasible in all procedures. Co-registration of the CBCT to the CTA dataset is shown in [Fig. 1](#). [Figs. 2](#) and [3](#) demonstrate fusion guidance during the FEVAR and BEVAR procedures.

All variables were normally distributed. The mean total procedure time in the fusion group was 5.2 hours (95% CI 4.5–5.9 hours), which was significantly lower than the

control group (6.3 hours, 95% CI 5.4–7.2 hours, $p = .022$). The mean procedural iodinated contrast material dose in the fusion group was 159 mL (95% CI 132–186 mL) versus 199 mL (95% CI 170–229 mL) in the control group. This difference was also significant ($p = .037$). Concerning fluoroscopy time, complete data could be retrieved for 11 pairs of fusion and case–control procedures. The average fluoroscopy time of the fusion group (50 minutes and 26 seconds, 95% CI 30:33–70:18) and case–control group (59 minutes and 29 seconds, 95% CI 40:40–78:19) were not significantly different ($p = .38$). [Table 2](#) provides a detailed overview of the objective outcome parameters of the fusion and case–control FEVAR/BEVAR procedures.

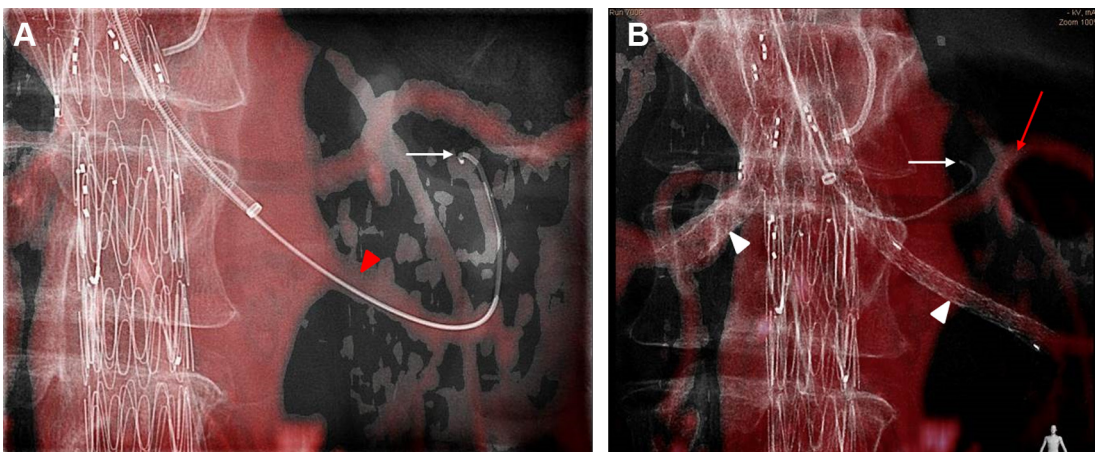


Figure 3. Fusion image guidance for left renal artery (A) and celiac trunk (B) catheterization from a transbrachial approach. Tip of the guidewire (white arrows) in the left renal artery (red arrow head) and splenic artery (red arrow) respectively. Covered stents in both renal arteries (white arrow heads).

Table 2. Iodinated contrast volume, procedure time and fluoroscopy time in fusion and case–control procedures.

ID Fusion — case–control	Iodinated contrast volume (mL)		Total procedure time (h)		Fluoroscopy time (min:s)	
	Fusion	Case–Control	Fusion	Case–Control	Fusion	Case–Control
1 – 32	160	NA	6	7.5		
2 – 33	110	250	4.5	11		
3 – 34	180	150	10	4.5		
4 – 35	200	250	7.75	10.25		
5 – 36	180	150	3.75	4		
6 – 37	200	250	5.25	5.75		
7 – 38	200	120	5.75	6		
8 – 39	125	325	7	8		
9 – 40	100	350	9	10		
10 – 41	75	80	7	8	93:41	NA
11 – 42	100	120	6	3	NA	71:02
12 – 43	Conversion	250	Conversion	8	Conversion	NA
13 – 44	150	250	7.5	8	59:58	NA
14 – 45	275	100	5	8.25	55:00	97:00
15 – 46	200	250	3	7.5	39:29	NA
16 – 47	90	220	3.25	5.5	26:42	NA
17 – 48	90	300	4.5	5	97:34	118:24
18 – 49	145	175	3.5	5	46:03	NA
19 – 50	225	150	5.25	3	81:12	57:38
20 – 51	200	270	5	5.5	42:21	58:00
21 – 52	320	250	4.5	8.5	84:29	51:00
22 – 53	120	125	4.5	6	45:41	61:39
23 – 54	200	150	7	6.25	111:13	NA
24 – 55	140	130	4.25	8	14:45	65:53
25 – 56	80	200	3.75	3.5	20:53	44:38
26 – 57	90	100	2.5	3	25:56	47:05
27 – 58	300	300	6	10.25	94:47	NA
28 – 59	100	220	3	2	16:19	38:52
29 – 60	160	300	4.5	6	70:32	14:13
30 – 61	240	150	5	6	85:47	NA
31 – 62	25	100	3	3	30:09	NA
Mean	159	199	5.2	6.3	50:26	59:29
Standard deviation	71	78	1.8	2.4	29:35	28:01

Note. Mean and standard deviation calculated only for pairs with complete data. NA = data not available.

Overlay inaccuracy

To some extent, fusion image overlay inaccuracy was observed during all procedures and was grouped into three main categories.

1. Overlay inaccuracy due to differences between CTA and CBCT acquisition.

The average time interval between acquisition of the diagnostic CTA and acquisition of the CBCT on the date of elective custom-made endograft repair was approximately 3 months. No overlay inaccuracies were observed due to these intervals. However, a mismatch between the pre-acquired CTA images and live fluoroscopy due to respiration-related vessel displacement was observed in all patients. In our clinic, diagnostic CTA scans are performed during breath-hold inspiration: a condition which is not typical for general anesthesia with low tidal volume ventilation. Respiration-related vessel mismatch was mainly observed at the level of the aortic arch and peripheral segments of the visceral branches. In Fig. 3, the mismatch between the tip of the guidewire and

the CTA overlay road-map in a distal section of the renal and splenic arteries is visible.

2. Overlay inaccuracy due to rigid co-registration.

Straightening and deformation of the vessel tree by stiff guidewires and stiff introduction devices was observed in 20 cases, mainly at the level of tortuous iliac arteries and distal elongated descending thoracic aorta. As co-registration with the pre-acquired CTA was performed in a rigid, non-elastic manner, any deformation of the vessel tree resulted in non-eradicable overlay inaccuracy during maneuver with stiff devices. Fig. 4 visualizes vessel deformity during graft introduction resulting in temporary overlay inaccuracy of the non-elastic fusion road-map.

3. Overlay inaccuracy due to patient movement

Any patient movement after CBCT acquisition resulted in overlay inaccuracy to the same extent and in the same direction as the original movement. As patients were under general anesthesia during the intervention, and CBCT was acquired immediately before vascular access, inaccuracy due to patient

movements was only observed if patients were repositioned by the surgical team. In the two cases, overlay mismatch could be eradicated by manual readjustment of the fusion road-map.

Complications

A complication was observed during the procedure of patient no. 12. While achieving access to the target vessel through the branch of the right renal artery, the guidewire and catheter were incorrectly positioned in the right colic artery (RCA). With the single plane C-arm in the anterior–posterior position and radiation protection shields covering the right flank, the superposition was neither detected on conventional angiogram nor on the fusion road-map. Deployment of the covered stent grafts obstructed the superior mesenteric artery distal to the RCA orifice with the need for surgical stent removal from the RCA and performance an iliac-superior mesenteric artery bypass. No major complications from the conversion have occurred. The patient has refused to undergo a second procedure connecting the renal and celiac branch to their target vessels.

DISCUSSION

The use of multimodality image fusion road-mapping in routine practice of complex endovascular aortic repair was evaluated. The data from the presented case–control study demonstrates that CTA with fluoroscopy fusion technology

results in significant reduction in procedure time and iodinated contrast material volume. A trend towards lower procedural fluoroscopy time was observed. Significant reduction of contrast material volume ($p = .001$) by means of fusion image road-mapping in complex EVAR has been described previously by Dijkstra et al.⁵ and Tacher et al.⁶ A single case of zero-contrast TEVAR using fusion has also been reported.⁴ Fenestrated and branched stent graft technology makes it possible to perform endovascular repair for complex aortic disease. Conventionally performed FEVAR/BEVAR is associated with a significant risk of adverse renal events due to the large volumes of contrast material used.^{7,8} Any effort and technology supporting a reduction in the volume of contrast material used is therefore highly relevant. Fusion image road-mapping promises significant benefits for vascular patients. However, there are some limitations of this technology and safety aspects that need to be discussed.

In our study, at all critical steps during the procedures, conventional angiograms were performed to confirm the correct position of the devices. This allowed us to get acquainted with fusion road-mapping and gain confidence with the new technology. In these procedures, contrast injections and procedure time were mainly reduced by more efficient target vessel catheterization under fusion road-map guidance. This provided a valuable benefit reflected in the results of our study. Nevertheless, this benefit is small compared with stent graft deployment used solely on the basis of the fusion road-map. With growing

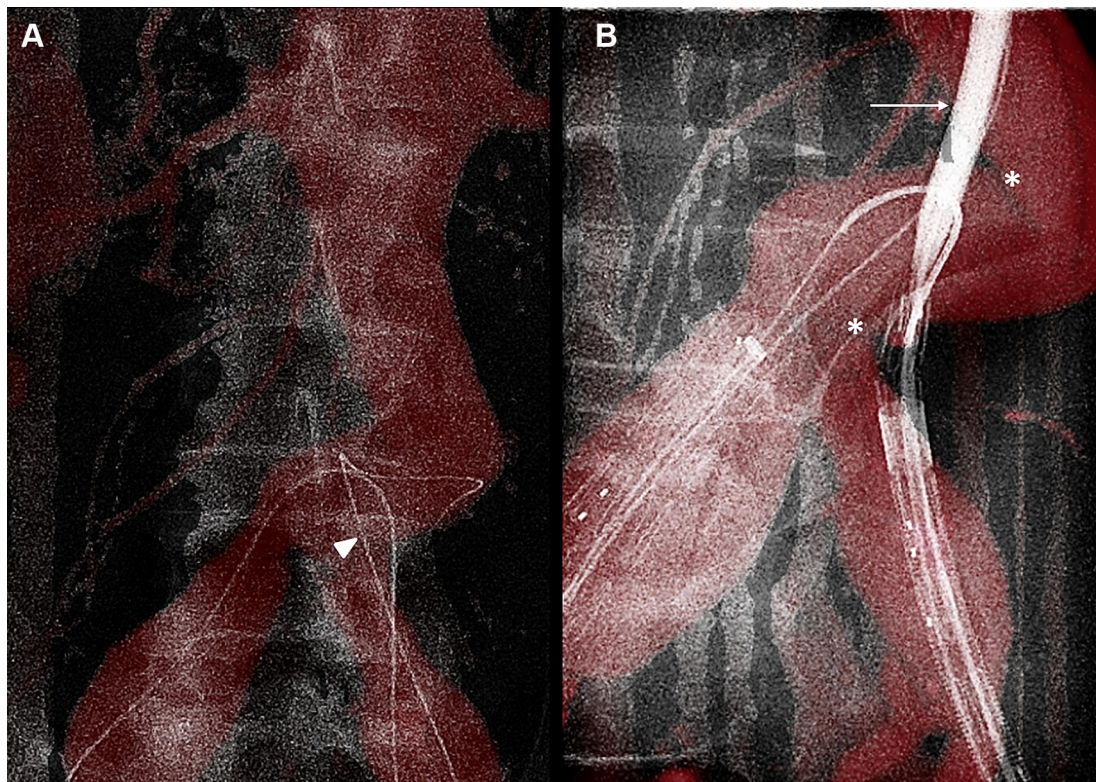


Figure 4. Fusion road-map overlay accuracy (A) with guide wires (white arrow head) precisely matching the vessel tree. Temporary local fusion overlay inaccuracy (B) during introduction of the stiff graft device (white arrow) at level of kinking elongated vessel tree (white asterisks) due to rigid image co-registration.

experience, in the last procedure, the aortograms prior to successful main device deployment under fusion guidance were omitted. It is however important to note that the amount of contrast volume saved due to the omitted aortograms is of trivial importance compared with the potential complication of a misplaced fenestrated device. In order to rely fully on fusion road-mapping, practical experience and precise knowledge of the limitations and accuracy errors of this technology are of critical importance. Inaccuracies of the overlay road-map were observed to some extent in all procedures, with respiration-related vessel displacement and temporary straightening of elongated vessels during maneuver with stiff devices being the most frequent. However, these inaccuracies may not hamper use of the fusion road-map provided the error and its range become predictable. Inaccuracies in locating peripheral segments of vessels due to organ movement corresponding to respiration-related diaphragm movement do not limit the use of the fusion road-map as long as the origin of the target vessels does not change position. In the fusion road-map accuracy analysis during EVAR from Fukuda et al.,¹⁰ the mean error of renal artery origin overlay image was 2 ± 2.5 mm, with a range from 0 to 7 mm. Further precise analyses of anatomy, respiration, and related overlay error are necessary to provide quantified predictions of overlay accuracy and expected extent of possible displacement. With growing experience and trust, further significant reductions of iodinated contrast volume and radiation exposure is to be expected.

There are limitations due to our study design. In the setting of advanced endovascular repair, procedure complexity and therefore procedure time, iodinated contrast volume and radiation dose are influenced by stent graft complexity. A case–control design with matching pairs based on stent graft complexity was therefore chosen. Controls were retrieved from a large pool of primarily historical procedures. This implies risk of bias in control selection as well as bias due to differences in operator experience. Controls had to most accurately technically match the fusion procedures; in the fusion group, the total number of fenestrations was slightly higher than the control group (Table 1). When there was more than one matching control, controls were prioritized by procedure date and only included procedures after 2010 aiming to minimize effects of experience level on our results. In this clinic more than 150 FEVAR and BEVAR procedures have been performed since 2006, all carried out by the same two specialists. Assuming that the learning curve after 2010 might already have flattened, experience gain during the procedures included in this study was expected to have minor influence on the significance of our results. Since 2010, there have been no changes in operation protocol and time registration that could have influenced our results. However, prospective randomized controlled studies evaluating fusion guidance are lacking but are needed. Furthermore, in future studies, radiation exposure should be focused. Multimodality image co-registration is possible by means of performance of a C-arm CBCT system. With the surgical

team usually outside the operation theater during acquisition, CBCT does not result in additional radiation exposure for the medical staff. However, patients undergoing CBCT are exposed to an extra load of radiation, in our study in the range between 0.5 and 2.6 mGy², depending on body length and weight. The total DAP of fenestrated and branched endovascular aneurysm repair procedures has been described in the range of 1–78 mGy².⁹ The case control pairs were not matched for body characteristics. Procedural DAP is influenced by patients' body mass index and further non-comparable between all procedures due to a software update of our hybrid fluoroscopy unit intended to shift radiation dose to a lower level. Considering this, the protocol was altered to compare fluoroscopy time, which is not influenced by body size and fluoroscopy units filters but indirectly reflects radiation exposure. Mean fluoroscopy time was on average 9 minutes lower in the fusion group. However, complete data could only be provided for 11 pairs for this variable. This limitation might have resulted in this observation not reaching statistical significance. Nevertheless, any reduction in fluoroscopy time is still relevant as it results in effective radiation dose reduction for the medical staff. A significant reduction of fluoroscopy time by use of fusion road-mapping might equalize patients' total procedural radiation exposure or even be decreased by fusion technology. In conclusion, further research evaluating influence of fusion guidance on fluoroscopy time and procedural radiation dose is needed.

There was one complication in the group of fusion patients. Due to superposition of vessels on the single plane view, catheter malposition was not recognized. In this respect, fusion road-map did not show superiority in terms of safety compared with conventional angiography. As volumetric CTA datasets are registered, any further improvement of the technology to provide real-time three-dimensional views would be beneficial and could address these actual limitations of two-dimensional fusion road-mapping.

Technical requirements for fusion guidance are a CBCT-feasible fluoroscopy unit as well as dataset co-registration software. Flat panel detectors that can acquire rotational 3D images, such as CBCT, have begun to replace conventional fluoroscopy units and co-registration software for image fusion is commercially available from different vendors. In our experience, time for CBCT acquisition was approximately 5 minutes and image co-registration was carried out while further preparations of the patient took place. Actual time loss for fusion set up was therefore negligible. For fusion guidance, semi-automated or automated removal of bones and other radiodense non-vascular structures should be performed on CTA datasets to avoid over-projection on the vessel tree overlay image.

In conclusion, fusion image guidance provided added value for FEVAR/BEVAR procedures in terms of procedure time and contrast volume reduction. Further application of this new technology to less complex but high volume routine procedures, for example peripheral artery

interventions might alter experience and further enhance procedural safety, for patients and surgeons.

CONFLICT OF INTEREST

None.

FUNDING

None.

REFERENCES

- 1 Abi-Jaoudeh N, Kruecker J, Kadoury S, Kobeiter H, Venkatesan AM, Levy E, et al. Multimodality image fusion-guided procedures: technique, accuracy and applications. *Cardiovasc Intervent Radiol* 2012;**35**:986–98.
- 2 Klein AJ, Tomkowiak MT, Vigen KK, Hacker TA, Speidel MA, Vanlysel MS, et al. Multimodality image fusion to guide peripheral artery chronic total arterial occlusion recanalization in a swine carotid artery occlusion model: unblinding the interventionalist. *Catheter Cardiovasc Interv* 2012;**80**:1090–8.
- 3 Glöckler M, Halbfäß J, Koch A, Achenbach S, Dittrich S. Multimodality 3D-road-map for cardiovascular interventions in congenital heart disease – a single-center, retrospective analysis of 78 cases. *Catheter Cardiovasc Interv* 2013;**82**:436–42.
- 4 Kobeiter H, Nahum J, Becquemin JP. Zero-contrast thoracic endovascular aortic repair using image fusion. *Circulation* 2011;**124**:e280–2.
- 5 Dijkstra ML, Eagleton MJ, Greenberg RK, Mastracci T, Hernandez A. Intraoperative C-arm cone-beam computed tomography in fenestrated/branched aortic endografting. *J Vasc Surg* 2011;**53**:583–90.
- 6 Tacher V, Lin M, Desgranges P, Deux JF, Grünhagen T, Becquemin JP, et al. Image guidance for endovascular repair of complex aortic aneurysms: comparison of two-dimensional and three-dimensional angiography and image fusion. *J Vasc Interv Radiol* 2013;**24**:1698–706.
- 7 Lindholt JS. Radiocontrast induced nephropathy. *Eur J Vasc Endovasc Surg* 2003;**25**:296–304.
- 8 Haddad F, Greenberg RK, Walker E, Nally J, O’Neill S, Kolin G, et al. Fenestrated endovascular grafting: the renal side of the story. *J Vasc Surg* 2005;**41**:181–90.
- 9 Maurel B, Sobocinski J, Perini P, Guillou M, Midulla M, Azzaoui R, et al. Evaluation of radiation during EVAR performed on a mobile c-arm. *Eur J Vasc Endovasc Surg* 2012;**43**:16–21.
- 10 Fukuda T, Matsuda H, Doi S, Sugiyama M, Morita Y, Yamada M, et al. Evaluation of automated 2D-3D image overlay system utilizing subtraction of bone marrow image for EVAR: feasibility study. *Eur J Vasc Endovasc Surg* 2013;**46**:75–81.